We obtained rate constants for some of the transfer reactions by using the usual techniques for reversible kinetics.[6] In the first two reactions in Table III the forward reaction proceeds with nearly unit collision efficiency, which suggests that the internal H bond is indeed formed within the lifetime of the reaction complex of the transfer reaction.

The third reaction in Table III constitutes an interesting case in that the forward reaction is exothermic but endoergic, while the reverse reaction is endothermic but exoergic. An unusual result is observed in that here the reverse, i.e., *endothermic reaction proceeds with nearly unit collision efficiency*. The present result is to our knowledge the first case where an endothermic reaction proceeds essentially at the collision rate.

Acknowledgment. This work was supported by Grant CHE77-14617 from the National Science Foundation.

Resonance Raman Spectra of Bacteriochlorophyll and Its Electrogenerated Cation Radical. Excitation of the Soret Bands by Use of Stimulated Raman Scattering from H_2 and D_2

Therese M. Cotton,[1] Keith D. Parks, and Richard P. Van Duyne*

Contribution from the Department of Chemistry, Northwestern University, Evanston, Illinois 60201. *Received February 13, 1980*

Abstract: The development of a new experimental method for producing laser wavelengths in the Soret band region of bacteriochlorophyll (BChl) and its electrogenerated cation radical permits a more detailed study of the effect of excitation wavelength on the resonance Raman (RR) spectrum than was previously possible. Stimulated Raman scattering (SRS) from H_2 or D_2 under high pressure is driven with the second or third harmonics of a Nd:YAG laser. Wavelengths ranging from 396.7 to 502.9 nm are generated. The highest energy wavelength is on the shoulder of the strongest Soret transition in neutral BChl. Good quality RR spectra are obtained at this wavelength, and no evidence of photodegradation is observed. In the case of BChl cation radical, however, the effect of excitation wavelength is more dramatic because it is possible to excite near resonance with three different intense electronic transitions by using the available laser lines. In addition, the resulting spectra show clearly that one-electron oxidation of BChl causes distinctive changes in its RR spectrum. Two intense RR bands seen in the $BChl^{+}\cdot$ spectrum are absent (1414 cm^{-1}) or only weakly observed (1340 cm^{-1}) in the corresponding spectra for BChl. These results indicate that selective RR monitoring of the formation and decay kinetics of the cation radical in vivo should be possible by using 416.0-nm excitation together with detection of the 1414- or 1340-cm^{-1} Raman peaks. The RR spectra of BChl and $BChl^{+}\cdot$ are examined in terms of recent ab initio configuration interaction calculations regarding the nature of the electronic transitions in the Soret region. The resonance enhanced Raman spectra agree qualitatively with changes in the molecular geometry which might be expected on the basis of the molecular orbital composition of the excited electronic state relative to the ground state.

Introduction

In the primary photochemical event of photosynthesis it is believed that a complex of two chlorphylls (Chl) or bacteriochlorophylls (BChl), denoted the special pair, undergoes one-electron oxidation to a π-cation radical in which the remaining unpaired electron is delocalized over both molecules of the complex.[2] The fate of the photoejected electron has been the subject of extensive research aimed toward elucidating the mechanism of photoinduced charged separation in plants. From picosecond absorption spectroscopy[3] and electrochemical studies[4] of photosynthetic bacteria as well as the isolated reaction center (RC) pigments, it appears that the electron is first transferred to an intermediate electron acceptor, bacteriopheophytin (BPheo), resulting in the formation of $BPheo^{-}\cdot$ with a lifetime of approxmately 250 ps. The $BPheo^{-}\cdot$ then transfers the electron to what has been termed the primary electron acceptor, a quinone–iron complex.[5,6] Besides the two special pair BChls and the BPheo intermediate, the RC complex contains two additional BChl molecules, called P800, and one additional BPheo. The role, if any, of these remaining pigment moieties in charge separation is uncertain at present. There is some evidence from picosecond time resolved absorption spectroscopy[7] and steady-state optical spectra of RC preparations at low redox potentials[8] that one of the P800 BChl's is also present as its anion radical. However, additional experiments are needed to determine if P800 BChl functions as an intermediate electron acceptor prior to BPheo as has been postulated.[7]

The progress which has been made toward understanding RC photochemistry can be largely attributed to three spectroscopic techniques–electronic absorption, ESR, and ENDOR spectroscopy—which have been used in conjuction with electrochemical,[4,9] potentiometric,[10] or photochemical[11] procedures for generating the cation and/or anion radicals of the photosynthetic pigments, either in solution or in the RC. Each of these spectroscopic approaches, while providing valuable information, has limitations. In the case of absorption spectroscopy, the spectra of $BChl^{-}\cdot$ and $BPheo^{-}\cdot$ in organic solvents have been used on a

(1) NIH Fellow, 1979.
(2) Norris, J. R.; Katz, J. J. In "Photosynthetic Bacteria"; Clayton, R. K.; Sistrom, W. R., Eds.; Plenum Press: New York, 1978, pp 397–418 and references therein.
(3) Holten, D.; Windsor, M. W. *Ann. Rev. Biophys. Bioeng.* **1978**, *7*, 189–227 and references therein.
(4) Fajer, J.; Brune, D. C.; Davis, M. S.; Forman, A.; Spaulding, L. D. *Proc. Natl. Acad. Sci. U.S.A.* **1975**, *72*, 4956–4960.
(5) Loach, P. A.; Hall, R. L. *Proc. Natl. Acad. Sci. U.S.A.* **1972**, *69*, 786–790.
(6) Feher, G.; Okamura, M.; McElroy, J. D. *Biochim. Biophys. Acta.* **1972**, *267*, 222–226.
(7) Shuvalov, V. A.; Kelvanik, A. V.; Sharkov, A. V.; Matveetz, Ju. A.; Krukov, P. G. *FEBS Lett.* **1978**, *91*, 135–139.
(8) Tiede, D. M.; Prince, R. C.; Dutton, P. L. *Biochim. Biophys. Acta* **1976**, *449*, 447–467.
(9) Dryhurst, G. "Electrochemistry of Biological Molecules"; Academic Press: New York, 1977; pp 408–415 and references therein.
(10) Prince, R. C.; Dutton, P. L., ref 2, pp 439–453 and references therein.
(11) Clayton, R. K., ref 2, pp 387–396 and references therein.

0002-7863/80/1502-6399$01.00/0

comparison basis to identify these species in vivo. An exact correspondence between the solution and in vivo spectra is not observed, however, because of sizable shifts in many of the absorption bands of BChl and BPheo in vivo.[12] Moreover, molecular information is difficult to extract from broad absorption bands of complex molecules such as the porphyrins. In contrast, ESR and proton ENDOR spectroscopy have provided substantial information regarding the electronic structure of the ground state of the radical ions.[13] Unfortunately, ESR and ENDOR spectra of $BChl^{-}\cdot$ and $BPheo^{-}\cdot$ are indistinguishable and cannot be used to identify the intermediate electron acceptor(s).[14] Also, the time resolution of the magnetic resonance techniques is limited to nanoseconds and, therefore, cannot be used to monitor directly picosecond events in photosynthesis.

In view of the above limitations, it is apparent that a new experimental approach is needed in photosynthetic studies which can provide the time resolution of absorption spectroscopy and the information content of ESR and ENDOR spectroscopy as well as a greater degree of molecular specificity than is now possible. Resonance Raman spectroscopy (RRS) has the potential for meeting these criteria. Its advantages have been cited frequently[15] and those most relevant to photosynthesis research are as follows: (1) sensitivity, (2) selectivity, (3) specificity, (4) versatility, and (5) temporal resolution. The large extinction coefficients of the porphyrins permit spectra to be recorded at very low concentrations (10^{-6}–10^{-4}) or well below the physiological concentrations. Moreover, the chlorophylls which differ in molecular structure (e.g., Chl a and Chl b) or function (e.g., antenna and RC's) have unique absorption spectra which should allow selective excitation of the RR spectrum of a particular class of chlorophylls in vivo. In green plants it has already been shown that it is possible to excite RR scattering from either Chl a or Chl b.[16] The high degree of specificity inherent in RRS is apparent from the distinctive spectra of BChl a and BPheo a in RC preparations.[17] These cited studies also illustrate the versatility of RRS. Spectra can be recorded on intact biological samples under a variety of sampling conditions. Finally, since RR scattering occurs in fractions of a picosecond, kinetic monitoring of primary events in photosynthesis is possible, at least in principle. There have been reports of nanosecond time-resolved RR studies on biological samples,[18,19] and very recently RR spectra have been obtained in the picosecond time domain.[20]

The application of RRS to the identification of radical ion intermediates in the RC of photosynthetic bacteria and time-resolved RRS to monitoring their formation and decay kinetics was first suggested by Cotton and Van Duyne.[21] In the RC complex neutral BChl and BPheo, the special pair BChl cation radical, and the intermediate electron acceptor(s) all have unique absorption bands. Therefore, laser excitation frequencies can be chosen to coincide with a particular absorption band in an individual molecule or its radical ion, thereby enhancing RR scattering from that species only. This is a decided advantage over electronic absorption spectroscopy, where the identification of a particular intermediate requires the use of difference techniques to separate out its contribution to the complex spectrum. However, in order to establish the feasibility of this approach, it is necessary to identify first the RR spectra of each of the possible radical ion intermediates individually in solution and to demonstrate that their vibrational spectra are sufficiently distinctive to enable their identification in the presence of the other RC molecules. For this purpose, resonance Raman spectroelectrochemistry (RRSE) was used in a preliminary study of BChl and its cation radical.[21] This technique, developed for the study of radical ions, uses electrochemical procedures for oxidizing or reducing the molecule under study.[22-24] Electrochemical methods are superior to chemical methods for redox purposes because it is possible to obtain quantitative yields without the use of extraneous oxidants or reductants which could contribute to the Raman spectrum or undergo further reactions with the radical ion under laser irradiation.

The results of the preliminary study of BChl and its cation radical by RRSE have shown that their vibrational spectra are indeed distinct.[21] However, at the time of that study, only a limited number of laser lines were available for excitation of the RR spectrum of these molecules. The highest energy line used, 457.9 nm of an Ar^{+} laser, is considerably lower in energy than the strong Soret transitions in either $BChl^{0}$ or $BChl^{+}\cdot$. In the case of $BChl^{+}\cdot$, the RR spectrum which resulted is unusual in that the intensity of the 1597-cm^{-1} band is dominant. This band was assigned to the 1609-cm^{-1} band of $BChl^{0}$ shifted to lower frequency on one-electron oxidation. A decrease in frequency results from a small decrease in bond order for those bands contributing to this normal mode (the methine C=C bonds). Other bands, which are observed in the 457.9-nm RR spectrum of $BChl^{0}$, were found to be relatively weak or absent (1530 and 1285 cm^{-1}) in $BChl^{+}\cdot$. The strong enhancement of only one normal mode in $BChl^{+}\cdot$ at this excitation wavelength was postulated to result from interference effects[25] and/or vibronic coupling[26] between two electronic states. In order to investigate these possibilities further, we needed RR spectra at multiple excitation wavelengths within and near the Soret bands in $BChl^{+}\cdot$. In the past, laser lines in this region of the electromagnetic spectrum were difficult to obtain. Presently, however, a new experimental approach[27] was used to produce a number of deep blue and violet lines by stimulated Raman scattering (SRS) from high-pressure H_2 or D_2. The use of SRS has enabled a more comprehensive investigation of the RR spectra of $BChl^{0}$ and $BChl^{+}\cdot$, resulting from Soret band excitation, than was previously possible. The results show conclusively that large differences exist between the spectra of these molecules at each of the wavelengths used. The RR spectrum of $BChl^{+}\cdot$ was found to be especially sensitive to excitation wavelength. Enhancement of unique vibrations at 1414 and 1340 cm^{-1} is observed when 396.7- and 416.0-nm light is used. These unique bands define, for the first time, experimental conditions for detecting $BChl^{+}\cdot$ in the presence of other photosynthetic species.

Experimental Section

BChl was isolated and purified according to standard procedures.[28] The potentiostat,[22] electrochemical cell,[29] and experimental method[21] used to prepare the cation radical have all been described.

An Ar^{+} laser (Coherent Radiation Model 52) was used as an excitation source for the CW RR spectra reported here. A description of the experimental apparatus used for obtaining pulsed spectra may be found in Van Duyne and Parks.[27] Briefly, the second (532 nm) and third (355

(12) Thornber, J. P.; Trosper, T. L.; Strouse, C. E., ref 2, pp 133–160 and references therein.

(13) Norris, J. R.; Scheer, H.; Katz, J. J. "The Porphyrins", Dolphin, D., Ed.; Academic Press: New York, 1978; Vol. IV, Part B, pp 159–195 and references therein. Fajer, J.; Davis, M. S.; Dolphin, D., *Ibid.* **1978**, *4B*, 197–256, and references therein.

(14) Okamura, M. Y.; Isaacson, R. A.; Feher, G. *Biochim. Biophys. Acta* **1979**, *546*, 394–417. Fajer, J.; Forman, A.; Davis, M. S.; Spaulding, L. D.; Brune, D. C.; Felton, R. H. *J. Am. Chem. Soc.* **1977**, *99*, 4134–4140.

(15) Van Duyne, R. P. *J. Phys. (Orsay, Fr.)* **1977**, C5-239–252.

(16) Lutz, M. *Biochim. Biophys. Acta* **1977**, *460*, 408–430.

(17) Lutz, M.; Kleo, J.; Reiss-Husson, F. *Biochem. Biophys. Res. Commun.* **1976**, *69*, 711–717.

(18) Woodruff, W. H.; Farquharson, S. *Science (Washington, D.C.)* **1978**, *201*, 831–833.

(19) Dallinger, R. F.; Nestor, J. R.; Spiro, T. G. *J. Am. Chem. Soc.* **1978**, *100*, 6251–6252.

(20) Dallinger, R. F.; Woodruff, W. H.; Rodgers, A. J. *Appl. Spectrosc.* **1979**, *33*, 522–523. Terner, J.; Spiro, T. G.; Nagumo, M.; Nicol, M. F.; El-Sayed, M. A. *J. Am. Chem. Soc.* **1980**, 102, 3238–3239.

(21) Cotton, T. M.; Van Duyne, R. P. *Biochem. Biophys. Res. Commun.* **1978**, *82*, 424–433.

(22) Jeanmaire, D. L.; Suchanski, M. R.; Van Duyne, R. P. *J. Am. Chem. Soc.* **1975**, *97*, 1699–1707.

(23) Jeanmaire, D. L.; Van Duyne, R. P. *J. Electroanal. Chem.* **1977**, *84*, 1–20.

(24) Jeanmaire, D. L.; Van Duyne, R. P. *J. Electroanal. Chem.* **1975**, *66*, 235–247.

(25) Zgierski, M. Z. *J. Raman Spectrosc.* **1977**, *6*, 53–56.

(26) Tsuboi, M.; Hirakawa, A. L.; Nishamura, Y. *J. Mol. Spectrosc.* **1977**, *68*, 335–358.

(27) Parks, K. D.; Van Duyne, R. P. *Opt. Lett.* submitted.

(28) Strain, H. H.; Svec, W. A. "The Chlorophylls"; Vernon, L. P., Seely, G. R., Eds.; Academic Press: New York, 1966; pp 21–66.

(29) Van Duyne, R. P.; Suchanski, M. R.; Lakovits, J. M.; Siedle, A. R.; Parks, K. D.; Cotton, T. M. *J. Am. Chem. Soc.* **1979**, *101*, 2832–2837.

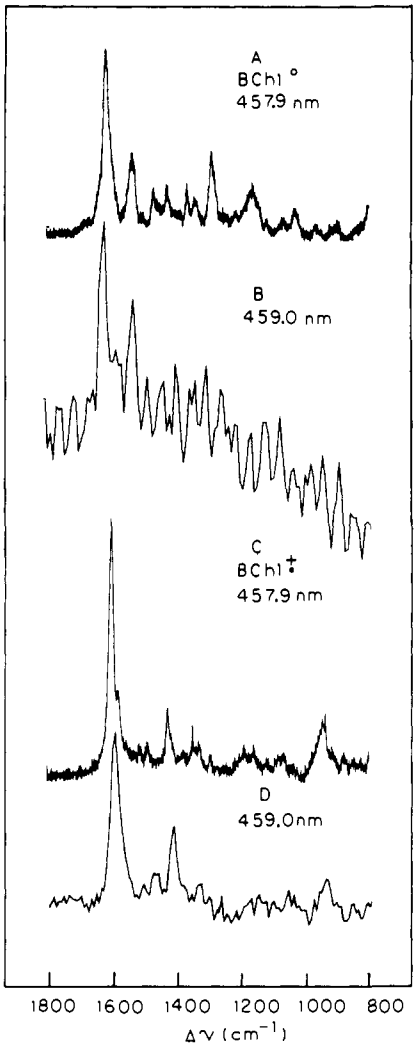

Figure 1. Comparison of CW (457.9 nm Ar^+, 30 mW) and pulsed (459.9 nm, 10 mW average power, 3000 pulses) resonance Raman spectrum of a 5×10^{-4} M solution of BChl neutral (A and B) and BChl cation radical (C and D) in CH_2Cl_2. Note scale for pulsed spectrum is slightly nonlinear and does not coincide exactly with the abscissa. This is because the vidicon detector is linear in wavelength, whereas the monochromator used in the CW experiments is linear in wavenumbers.

nm) harmonic from a flash lamp pulsed Nd:YAG (Quanta Ray Corporation Model DCR-1) equipped with angle turned type II KD*P harmonic crystals is focused into a stainless-steel cell (2.5 cm in diameter by 1 m in length) containing hydrogen or deuterium gas at 70 psi. The output beam, which is composed of the pump beam, stimulated Raman-shifted light, as well as Stokes and anti-Stokes components of the nonlinear process involving these two beams, is separated into its components by a quartz Pellin Broca prism. The desired wavelength is focused onto the sample by a 1000-mm focal length field lens followed by a 90-mm focal length cylindrical lens. Raman scattered light is collected in the backscattering mode.[22] An Astro–Berlin (focal length = 75 mm, F = 1.1) camera lens is used to focus the Raman scattered light onto the slits of a triple holographic grating spectrograph (Instruments SA Model DL-203). The spectrograph output is detected with an optical multichannel analyzer (PARC OMA-2) equipped with an uncooled SIT Vidicon Tube.

Results and Discussion

Stability of BChl and $BChl^{+\cdot}$ to High Peak Power Used in Pulsed Excitation. In the pulsed experiments the average power used to excite Raman scattering in the samples was 10 mW, corresponding to pulses of 1-mJ energy at 10-Hz repetition rate. Before beginning a detailed study of the RR spectra of BChl and its cation radical, it was necessary to determine the stability of these molecules to pulsed irradiation since there have been no previous RR studies of any of the chlorophylls utilizing pulsed excitation. The stability was monitored in three ways: (1) absorption spectra

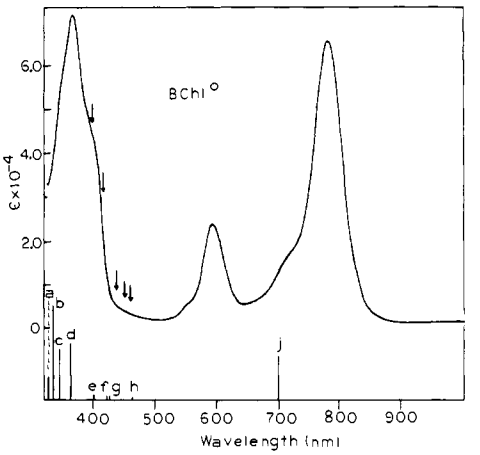

Figure 2. Electronic absorption spectrum of BChl neutral in CH_2Cl_2. Arrows indicate the position of laser excitation wavelengths used for resonance Raman spectroscopy. Lines below the spectrum are the calculated electronic transitions according to Petke et al.[31] The letters designate singlet states according to those authors' nomenclature: a = S_{12}, b = S_{11}, c = S_{10}, d = S_9, e = S_8, f = S_7, g = S_5, h = S_3, i = S_2, and j = S_1. The line heights are proportional to the calculated oscillator strengths.

were recorded on the samples before and after laser irradiation, (2) spectra were recorded at low power CW irradiation with the Ar^+ laser (457.9 nm, 10–20 mW) and compared with pulsed spectra obtained at approximately the same wavelength (459.0 nm), and (3) CW spectra were recorded on the same sample before and after recording pulsed spectra. In no case was there any evidence of irreversible photoreactions.

A distinction should be made, however, between irreversible photodamage which can be detected in our experimental procedure and that which is reversible. The latter may conceivably be present in both the CW and pulsed experiments, if an intermediate state is produced from the excited state of BChl (BChl*) which decays back to BChl*. In order to detect this hypothetical intermediate, one should study the pulsed RR spectrum as a function of pulse width and gating procedures should be employed to detect the Raman signal at precise time intervals following the excitation pulse. These experiments could not be performed at the present time and, hence, our data do not speak to the question of photoreversible intermediate states in BChl.

Figure 1 shows a comparison of the RR spectra of BChl neutral obtained using CW (A) and pulsed (B) excitation, as well as that of $BChl^{+\cdot}$ obtained by using CW (C) and pulsed (D) excitation. The basic similarity between the spectra in both cases indicates that the high peak powers used in the pulsed experiments do not produce detectable photodamage in either BChl or $BChl^{+\cdot}$. At these wavelengths, 457.9 and 459.0 nm, it might be argued that BChl and $BChl^{+\cdot}$ are not strongly absorbing (see Figures 2 and 5) and, therefore, are not as likely to suffer irreversible photodamage as would be the case at higher energy wavelengths, where their extinction coefficents are much larger. A comparison was made of the 457.9-nm CW RR spectrum with the 459.0-nm pulsed RR spectrum because these were the closest CW and pulsed lines available to us. (Indeed, the lack of available laser wavelengths, either CW or pulsed, in the region below 450 nm provided the impetus for our development of SRS as a Raman excitation source!) There is other experimental evidence which argues strongly against irreversible photodamage at the higher energy excitation wavelengths. This evidence includes the lack of change in the absorption and CW RR spectra of a given sample before and after the pulsed RR experiment and the lack of change in the intensities and peak frequencies in the pulsed RR spectrum with exposure time. The multiplex advantage of the OMA detection system undoubtedly assists in minimizing photodegradation of the samples in that it significantly reduces the exposure time of the sample to the laser beam relative to that required for recording spectra by conventional detection modes. In either CW or pulsed experiments, however, it is essential that the samples

Table I. Relationship between the Experimental and Calculated Electronic Transitions of BChl^0 and BChl$^{+\cdot}$ to Laser Excitation Frequencies[a,b,c]

laser excitation freq	electronic transition calcd[b]	electronic transition exptl
	BChl^0	
25 208 (396.7)	S_{11} 30 603 (326.8)	27 200 (368)
	S_{10} 29 338 (340.9)	25 300 (395)
	S_9 27 503 (363.6)	
24 038 (416.0)		
22 952 (435.7)	S_8 24 874 (402.0)	22 700 (440)
	S_7 24 185 (413.5)	
22 222 (450.0)		
21 786 (459.0)	S_3 21 485 (465.4)	
	BChl$^{+\cdot}$	
25 208 (396.7)	D_{26} 25 998 (384.6)	25 500 (392)
	D_{24} 25 782 (387.9)	
24 038 (416.0)	D_{23} 24 359 (410.5)	23 700 (422)
22 952 (435.7)		
22 222 (450.0)		
21 786 (459.0)	D_{17} 21 876 (457.1)	
19 885 (502.9)	D_{14} 19 285 (518.5)	19 900 (502)

[a] Frequency in inverse centimeters. Wavelength in nanometers is shown in parentheses. [b] According to Petke et al.[31,38] [c] Lines connecting laser excitation frequency to calculated electronic transition indicate probable coupling on the basis of RR results.

be rigorously degassed to prevent photooxidation.

RR Spectroscopy of BChl^0 and BChl$^{+\cdot}$ as a Function of Excitation Wavelength in the Soret Band. The use of SRS provides an opportunity to probe the Soret band of BChl and its cation radical. This is an important region of the BChl absorption spectrum for at least three reasons. First, the Soret band is sensitive to BChl interactions in vivo.[30] Second, excitation into the Soret region permits recording of the RR spectra of the photosynthetic pigments, since fluorescence emission, which would obliterate the RR spectra, is not strongly allowed from the higher energy transitions. Most fluorescence occurs from the lowest energy transition, or far to the red of the excitation frequency. Hence, the RR spectrum is in the window between the excitation band and the fluorescence emission. Third, a study of the RR spectrum as a function of excitation wavelength in the Soret offers the possibility of resolving the multiple overlapping electronic transitions. The experimental data provide valuable information regarding the bond distortions in the excited states which is extremely useful for comparison with theoretical descriptions of the electronic configurations of the excited states.

An examination of the experimental absorption spectra of BChl^0 (Figure 2) shows there are several overlapping transitions in the 460–300-nm region. Recent MO calculations have predicted there are seven transitions of strong to moderate oscillator strength and two extremely weak transitions (oscillator strength less than 0.04) in this region.[31] The predicted transitions are shown below the experimental spectrum in Figure 2. Table I lists the experimental transitions and, where possible, the correlations with the calculated values according to Petke et al.[31] are indicated. Laser excitation wavelengths are designated in Figure 2 and listed in Table I near the appropriate electronic transition.

The RR spectra of BChl^0 and BChl$^{+\cdot}$ for a series of excitation wavelengths produced by SRS from H_2 or D_2 will be discussed in terms of two regions: (A) 1800–1450 cm^{-1}—the Raman bands in this region have been ascribed predominantly to methine C=C double bond stretching motions from normal-mode analysis of highly symmetric prophyrins—and (B) 1450–950 cm^{-1}—this region contains normal modes with large contributions from the C–N bonds of the pyrrole rings.[32] In the case of BChl, the relative

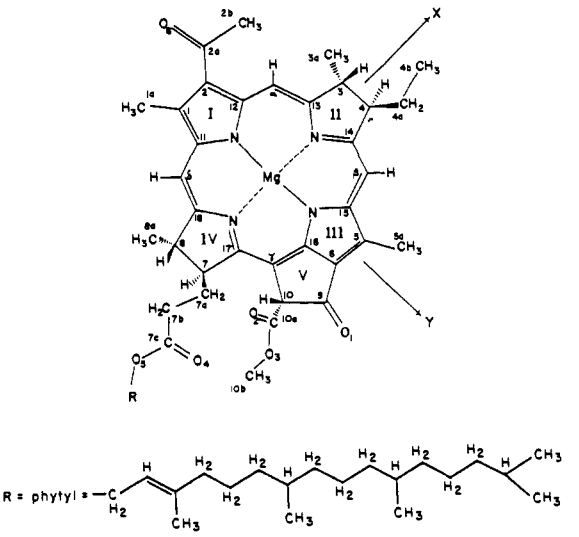

Figure 3. Molecular structure of BChl.

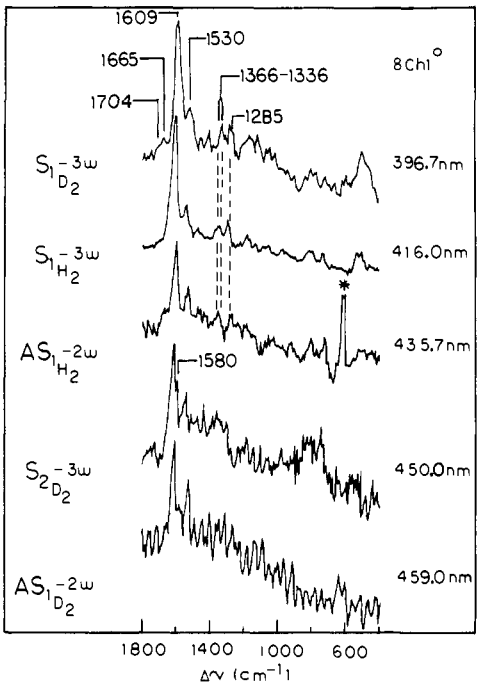

Figure 4. Pulsed resonance Raman spectrum of BChl neutral (10^{-2} M in CH_2Cl_2) as a function of excitation wavelength. Designation at left of RR spectra is that of Parks and Van Duyne.[27] For the origin of the SRS from either H_2 or D_2: s = Stokes shifted Raman light, as = anti-Stokes shifted Raman light, $n\omega$ = fundamental (n = 1) or higher (n = 2, 3) harmonic of Nd:YAG pump laser. Asterisks indicate artifacts.

contributions of specific bonds to the normal modes in both of these regions cannot be assigned at the present time. Undoubtedly, each band is a complex mixture of vibrations. There is some support, however, for similarities between the frequency and composition of the normal modes of symmetrical porphyrins with those of lower symmetry from the analysis of Solovyov et al.[33] Therefore, where possible, comparisons will be made between bands in BChl and those which have been assigned in other porphyrins. These comparisons are tentative—an unambiguous assignment of the RR vibrations in BChl will require isotopic substitution and normal mode analysis. The molecular structure and numbering system used for atomic designation in BChl are

(30) Weiss, C. "The Porphyrins", Dolphin, D., Ed.; Academic Press: New York, 1978; Vol. III, Part A, pp 211–223.
(31) Petke, J. D.; Maggiora, G. M.; Shipman, L. L.; Christoffersen, R. E. *Photochem. Photobiol.*, in press.
(32) Felton, R. J.; Yu, N.-T. "The Porphyrins", Dolphin, D., Ed.; Academic Press: New York, 1978; Vol. III, Part A, pp 347–393, and references therein.
(33) Solovyov, K. N.; Gladkov, L. L.; Gradyushko, A. T.; Ksenofontova, N. M.; Shulga, A. M.; Starukhin, A. S. *J. Mol. Struct.* **1978**, *45*, 267–305.

Table II. RR Vibrational Frequencies (cm^{-1}) of BChl in CH_2Cl_2 Using Pulsed and CW Excitations[a,b]

excitation wavelength (nm)					
396.7	416.0	435.7	450.0	457.0	459.0
1704		1698			
1673		1666		1665	
1611	1610	1608	1606	1609	1608
1580 (sh)	1590 (sh)	1584 (sh)	1580 (sh)	1592 (sh)	
1530	1533	1534	1531	1530	1534
1461	1466	1470		1465	
1414					
	1360	1366		1360	
1340	1350		1341	1336	
1286	1292	1289		1285	
1180	1174			1170	
	1155			1160	
1137	1130				
1083	1076			1087	
1061					
1028				1030	

[a] All excitation wavelengths shown excepting 457.9 (CW Ar^+) were obtained by using SRS from high-pressure H_2 or D_2. [b] Only bands which are well resolved from background noise are listed. sh = shoulder.

shown in Figure 3. Raman bands will be discussed in terms of the specified numbers and letters.

1. RR Spectroscopy of BChl[0]. Figure 4 shows a series of RR spectra for BChl as a function of excitation wavelength using the pulsed SRS from H_2 or D_2. The origin of the SRS is based on the notation of Van Duyne and Parks[27] and is listed next to the excitation wavelength. The vibrational frequencies are listed in Table II.

Small variations in a particular band frequency (less than 10 cm^{-1}) with excitation wavelength were not considered signficant. For simplicity, as well as accuracy, each band is discussed in terms of the frequency obtained by using 457.9-nm excitation, since the resolution was greatest under these experimental conditions.

(A) **1800–1450-cm^{-1} Region.** The highest energy excitation wavelength used in the present study, or 396.7 nm, is closest energetically to the 395-nm shoulder in BChl (S_9, S_{10}). It is also in preresonance with the stronger 368-nm absorption band (S_{11}). The vibrational spectrum may reflect coupling to all three of these electronic states, since the greater energy gap between the excitation wavelength and S_{11} is conceivably offset by its larger extinction coefficient relative to S_9 and S_{10}.

In the 396.7-nm spectrum shown in Figure 4, the most intense feature is the 1609-cm^{-1} band. This and the second most intense band at 1530 cm^{-1} are due primarily to methine C=C vibrations. Weaker carbonyl vibrations are also seen at 1704 cm^{-1} (C_9 keto carbonyl) and 1665 cm^{-1} (C_2 acetyl carbonyl). As the excitation wavelength is shifted farther to the red in the Soret band, there is a decrease in overall signal intensity. In the pulsed spectra recorded at excitation wavelengths greater than 435.7 nm, the signal to noise ratio is very low. This is *partially* due to the decreased sensitivity of the vidicon detector at these higher wavelengths but is also due to the weaker coupling of the laser line with the intense Soret electronic states. The major changes observed in the RR spectrum as the excitation wavelength is moved to the red include the following: (1) a loss of the carbonyl modes in the 416.0-nm spectrum and their reappearance in the 435.7-nm spectrum; (2) a steady decrease in the 1609-cm^{-1} band relative to the other bands; and (3) an increase in the intensity of the 1584–1580-cm^{-1} shoulder on the 1609-cm^{-1} band in the 435.7- and 450.0-nm spectra and a decrease in its intensity in the 459.0-nm spectrum.

(B) **1450–950 cm^{-1}.** Changes in this region of the RR spectrum with excitation are more difficult to assess. The bands are relatively weak and cannot be distinguished from the background noise in spectra obtained with wavelengths greater than 435.7 nm. The main changes include the following: (1) a band near 1414 cm^{-1} is observed in the 396.7-nm spectrum but is no longer distinguishable in spectra obtained at longer wavelengths; (2) several overlapping bands are seen between 1366 and 1336 cm^{-1}, which vary in intensity with excitation wavelength; and (3) a decrease in the relative height of the 1285-cm^{-1} peak is observed on exciting from the blue to the red region of the excitation spectrum. The bands near 1366–1336 cm^{-1} appear analogous to the 1360–1340-cm^{-1} oxidation state marker in hemes, which are thought to contain a sizable contribution from the C–N vibrations of the pyrrole rings.[34] In BChl, it may be that overlapping peaks in this region reflect normal modes composed of varying amounts of the four nonequivalent pyrrole C–N vibrations. The changes in the relative intensities of these peaks might then reflect coupling of the exciting wavelength to different electronic transitions in BChl. In the 396.7-nm spectrum, the major peak in this region is at 1340 cm^{-1}, whereas in the 416.0-nm spectrum there are two vibrations at 1360 and 1350 cm^{-1} of approximately equal intensity. Only the 1366-cm^{-1} peak is seen in the 435.7-nm spectrum. (The resolution under the experimental conditions used is ±5 cm^{-1}, and therefore, differences of ~5 cm^{-1} cannot be considered significant.) The band near 1285 cm^{-1} is close to the 1309-cm^{-1} peak in octaethylporphyrin (OEP) and is tentatively assigned to in-plane bending modes from the methine C–H bonds.[35] Vibrations between 1200 and 950 cm^{-1} appear very weak and overlap considerably. It is difficult to measure their frequencies and intensities with any accuracy, and therefore these bands will not be discussed.

Modes below 950 cm^{-1} in BChl are only weakly coupled to the Soret transitions, as is evident in all of the spectra shown in Figure 4. The region below 550 cm^{-1} contains broad featureless Raman background from the glass sample tube. This is especially apparent in the 396.7-nm spectrum, where the large extinction coefficient of BChl necessitates focusing the Raman collection lens near the surface of the sample tube. There are definite shoulders due to BChl RR scatter on the glass background, however, and it does appear that modes below 550 cm^{-1} are somewhat more intense with higher energy excitation (i.e., 396.7 nm vs. 435.7 nm).

As noted above, RR spectra contain information regarding bond order changes which occur in molecules on electronic excitation. A RR spectrum is usually considerably simpler than the normal Raman (NR) spectrum for a given molecule because, in the former, band intensities are governed by Franck–Condon factors. Those normal modes which undergo large changes in equilibrium nuclear configuration in the excited state, or are coupled to the electronic transition, are significantly (10^4–10^6) more intense than normal modes which undergo little or no distortion in the excited state. The latter exhibit only NR scattering and are obscured by the resonance enhanced bands. In addition, in RR scattering the magnitude of the enhancement is dependent upon the oscillator strength and the excited-state line widths of the electronic transition.[36] Thus, a detailed study of the effect of excitation wavelength on the intensity of various bands by RR excitation spectroscopy provides information concerning the electronic transitions and the vibrational frequencies of the excited state. An example of such a study is that of Jeanmarie et al.,[37] who examined the lowest $^2B_{1u}$ excited state of $TCNQ^-$· using a Rhodamine 6G dye laser to excite Raman scattering. In the present study, only six laser lines were available for excitation into the Soret band of BChl and its cation radical. Many more spectra are needed at closely spaced intervals in order to understand more fully this complex region of the absorption spectrum. Polarization data is needed to identify interference and vibronic coupling between the numerous electronic states. Nonetheless, it is useful to examine the present data in terms of the most recent theoretical interpretation of this region of the spectrum.

Petke et al.[31] have employed ab initio quantum mechanical procedures to determine the molecular orbitals for the ground-state

(34) Kitagawa, T.; Abe, M.; Kyogoku, Y.; Ogoshi, H.; Suzimoto, H.; Yoshida, Z. *Chem. Phys. Lett.* **1977**, *48*, 55–58.

(35) Kitagawa, T.; Ozaki, Y.; Kyogoku, Y. *Adv. Biophys.* **1978**, *11*, 153–196.

(36) Rousseau, D. L.; Friedman, J. M.; Williams, P. F. "Raman Spectroscopy of Gases and Liquids"; Weber, A., Ed.; Springer-Verlag: New York, 1979, pp 203–252 and references therein.

(37) Jeanmaire, D. L.; Van Duyne, R. P. *J. Am. Chem. Soc.* **1976**, *98*, 4029–4033.

SCF wave function. Using these molecular orbitals and configuration interaction (CI), they have further calculated low-lying singlet and triplet states in the absorption spectrum. The results are excellent in that many of the experimental spectral features are accounted for in the calculated spectrum. Of particular interest here are the transitions in the Soret band. The experimentally determined polarizations for the strongest transitions along the molecular axes (see Figure 3) are y-polarized (361 nm) and x-polarized (391 nm). The theoretical results predict identical polarizations. The probable correlations of the predicted transitions with the experimental are shown in Table I. Also shown is the relationship of the laser excitation line to the calculated and experimental transition. In this respect, it may be noted that the calculated transitions are at higher energy than the experimental. While this represents no problem in identifying the strong transitions, it does not allow an exact match of the laser excitation line with the weaker calculated transitions, as the latter are not observed in the experimental spectrum. With this uncertainty in mind, an attempt will be made to evaluate the RR changes in the $BChl^0$ spectrum with variation of the excitation wavelength from 396.7 to 450.0 nm on the basis of the theoretical description of the electronic states.

The RR spectrum of $BChl^0$ resulting from excitation at 396.7 nm is coupled to the calculated S_9 and S_{10} transitions. A description of the configuration of these transitions shows they contain extensive π-electron delocalization similar to that described in the "four orbital model" of the absorption spectrum (i.e., transitions occur between the two highest occupied and the two lowest unoccupied orbitals of the ground-state SCF wave function). The molecular orbitals involved in these transitions show considerable electron density at the methine carbons. From the RR spectrum it may be seen that vibrations attributed to the methines (1609 and 1530 cm^{-1}) are strongly enhanced at this excitation wavelength, indicating distortion of these bonds occurs in the excited state. Excitation at 396.7 nm is also in preresonance with the intense S_{11} transition at 361 nm. The configuration of this transition shows π-electron population at the C_2 acetyl and C's 5 and 6. The acetyl band at 1665 cm^{-1} arises, no doubt, from coupling to this state. A band near 1414 cm^{-1} may represent a normal mode containing the C=C vibrational from C's 5 and 6. Excitation at 416.0 nm is less strongly coupled to the S_{11} transition, as the acetyl and 1414-cm^{-1} bands are absent in the RR spectrum. The acetyl band is again observed in the 435.7-nm spectrum, which suggests coupling to the calculated S_7 and S_8 transitions. Both of these excited states involve π-electron density at the acetyl group. Since the exact position of these states is unknown relative to the experimental spectrum, it is not possible to say whether the 435.7-nm spectrum involves coupling to one or both of these transitions. Pulsed RR spectra obtained with 450.0-nm excitation are not yet of sufficiently good quality to make comparisons with theoretical calculations concerning the weak electronic transitions in this region.

2. RR Spectroscopy of $BChl^{+}\cdot$. A comparison of the experimental optical spectra of $BChl^{+}\cdot$ (Figure 5) with $BChl^0$ (Figure 2) illustrates the sizable changes which occur on removal of one electron from the highest occupied molecular orbital of the ground state. The lowest energy transition (D_3) which has been observed in $BChl^{+}\cdot$ is much weaker in oscillator strength than that in $BChl^0$ (S_1). In the Soret region (below 500 nm) there are two strong transitions which are well resolved. That near 422 nm results in particularly strong RR scattering from this state. Also, the better separation between the Soret transitions leads to more definitive changes in the RR spectrum of the cation radical with excitation wavelength than those observed for the neutral molecule, as may be seen in Figure 6. The vibrational frequencies are listed in Table III. As was noted in the case of the RR spectra of $BChl^0$, bands which are common to the pulsed and CW spectra are discussed in the text according to the values obtained by using 457.9-nm excitation. An exception to this is, of course, those bands which are unique to the higher energy pulsed excitation spectra.

(A) 1800–1450 cm^{-1}. There are two significant changes in the RR spectrum of $BChl^{+}\cdot$ with excitation wavelength in this region.

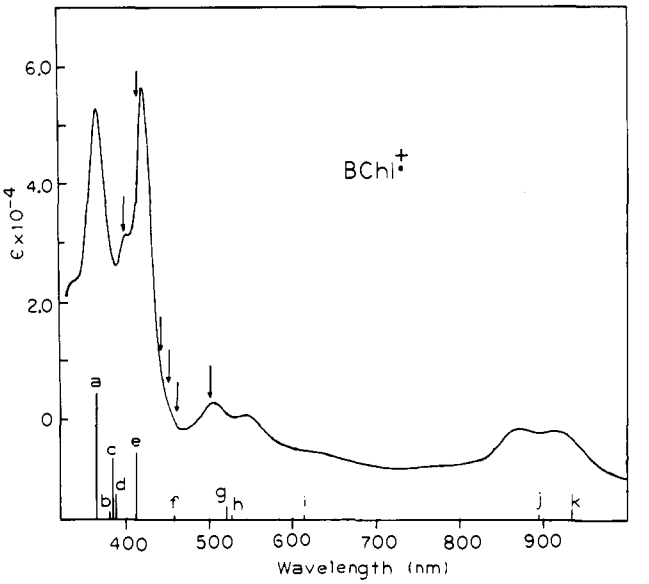

Figure 5. Electronic absorption spectrum of BChl cation radical in CH_2Cl_2. Arrows indicate the position of laser excitation wavelengths used for resonance Raman spectroscopy. Lines below the spectrum are the calculated electronic transitions according to Petke et al.[38] The letters designate doublet states according to these authors' nomenclature: a = D_{28}, b = D_{27}, c = D_{26}, d = D_{24}, e = D_{23}, f = D_{17}, g = D_{15}, h = D_{14}, i = D_{11}, j = D_5, and k = D_3. The line heights are proportional to the calculated oscillator strengths.

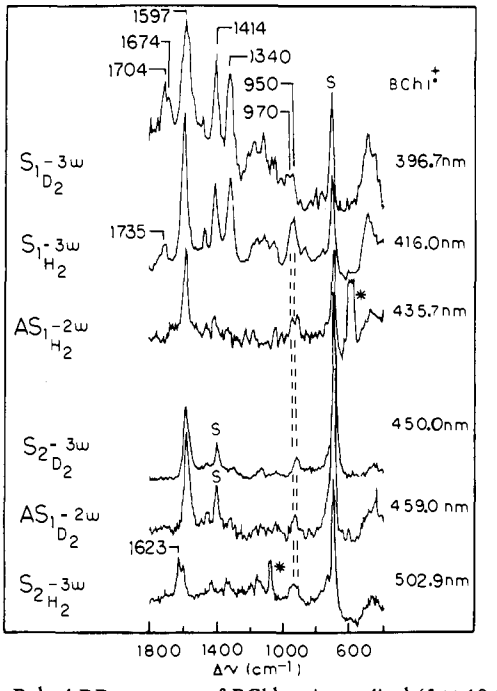

Figure 6. Pulsed RR spectrum of BChl cation radical (5×10^{-4} M in CH_2Cl_2) as a function of excitation wavelength. Designations in this figure are identical with those in Figure 4.

First, excitation at 396.7 nm produces an intense band at 1597 cm^{-1} identical with that observed previously with 457.9-nm light.[21] This peak has been assigned to the low frequency shifted methine C=C vibration which occurs at 1609 nm^{-1} in $BChl^0$. A decrease in vibrational frequency indicates a decrease in the ground-state bond order for those bonds contributing to this normal mode. Large spin density changes are calculated for C's in the vicinity of the methines on one-electron oxidation of BChl, and, therefore, the observed changes are consistent with these calculations.[38] On

(38) Petke, J. D.; Maggiora, G. M.; Shipman, L. L.; Christoffersen, R. E. *Photochem. Photobiol.* **1980**, *31*, 243–257.

Table III. RR Vibrational Frequencies of $BChl^{+\cdot}$ in CH_2Cl_2 Using Pulsed and CW Excitations[a,b]

excitation wavelength							
396.7	416.0	435.7	450.0	457.0	459.0	502.9	
	1735 (sh)						
1704	1703						
1683 (sh)	1671 (sh)					1623	
1591	1596	1596	1594	1597	1600	1596	
1570 (sh)	1568 (sh)	1560 (sh)		1578 (sh)	1580 (sh)	1576 (sh)	
1487	1487	1480	1482	1482	1481		
1414	1417	1425*	1420*	1427*	1421*	1423*	
				1374			
1340	1335			1345	1345	1338	
1329 (sh)			1326 (br)	1322		1320	
1297 (sh)			1286 (vw)	1288			
		1246					
1223							
1190	1195	1202	1206				
1180			1182	1187			
	1166		1165	1161		1156	
1137	1127					1127 (sh)	
				1113			
1071	1067	1070		1070	1068		
				1063			
1028		1026		1031			
984				973		980	not resolved
	970	963		957		970	
952	950	936	952	950	950	950	

[a] All excitation wavelengths shown except 457.9 (CW Ar^+) were obtained by using SRS from high-pressure H_2 or D_2. [b] Only bands which are well resolved from background noise are listed. sh = shoulder, br = broad, and * = solvent band.

excitation farther to the red (416.0 nm) the intensity of the 1597-cm^{-1} band is observed to increase relative to the solvent (CH_2Cl_2) band at 718 cm^{-1} and then decrease (435.7 nm and farther to the red). A plot of intensity versus excitation wavelength for the 1597-cm^{-1} band as well as several others in $BChl^{+\cdot}$ is shown in Figure 7. Although the number of points in this plot is limited, it may be seen that the maximum intensity for the 1597-cm^{-1} peak is observed with 416.0-nm excitation, indicating this vibration is strongly coupled to the 422-nm transition in the absorption spectrum. In the 502.9-nm RR spectrum, a splitting is observed in the 1597-cm^{-1} band, with another band of approximately equal intensity occurring at 1623 cm^{-1}. The spectrum is substantially different from that reported recently[39] for $BChl^{+\cdot}$ in methanol which was obtained by using 514.5-nm excitation. In this latter study, the cation radical was prepared by I_2 oxidation and the spectrum was recorded at 30 K. Hence, both the experimental conditions and the excitation wavelength were different from those used here. Since there are two overlapping electronic transitions in this region (D_{13} and D_{14})[38] involving orbitals with different configurations, a more detailed investigation of the RR spectrum of $BChl^{+\cdot}$ vs. excitation wavelength in the 500–530-nm region is needed.

The second major effect of excitation wavelength on the RR spectrum of $BChl^{+\cdot}$ in the 1800–1450-cm^{-1} region concerns the C=O stretching modes at 1704 and 1674 cm^{-1}. In the 396.7-nm spectrum the intensity of these bands is by far the greatest observed in either $BChl^0$ or $BChl^{+\cdot}$. As the excitation wavelength is moved to the red, the C=O intensities decrease. In the 416.0-nm spectrum, a new relatively weak shoulder is seen at 1735 cm^{-1}. This shoulder is due to resonance enhancement of one or both of the ester carbonyls in BChl (C's 7 and 10).

(B) 1450–950 cm^{-1}. The major features observed in this region of the RR spectrum of $BChl^{+\cdot}$ may be summarized as follows: (1) Two strong vibrations are observed at 1414 and 1340 cm^{-1} in the 396.7-nm RR spectrum. These are also strong in 416.0-nm spectrum, but their intensities fall off rapidly as the excitation wavelength is moved to 435.7 nm. Because of the decrease in signal to noise ratio, neither peaks can be unambiguously assigned in spectra recorded with excitation between 435.7 and 459.0 nm. The 1340-cm^{-1} peak is again observed, through with low intensity, in the 502.9-nm spectrum. (2) There are numerous overlapping bands in the 1250–1000-cm^{-1} region which decrease in intensity as the excitation wavelength progresses from 396.7 nm to the red. (3) Two overlapping bands at 968 and 948 cm^{-1} increase in intensity at 416.0 nm relative to 397.1 nm excitation, but then decrease on excitation at 435.7 nm. The two peaks are no longer resolved in the 450.0-nm spectrum; only one broad peak is seen at 952 cm^{-1}. On excitation at 502.9 nm, however, a series of poorly resolved peaks are again seen in this region.

The region near 800 cm^{-1} is obscured by the strong solvent peak at 718 cm^{-1}. As discussed in conjunction with the BChl neutral RR spectra, excitation at 396.7 and 416.0 nm produces a large Raman contribution from the glass cell making interpretation of the peaks below 550 cm^{-1} difficult. There are several shoulders

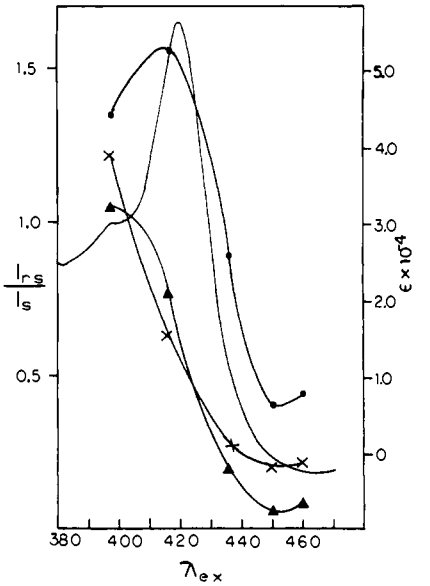

Figure 7. Excitation profiles for the 1596-cm^{-1} band (●), the 1414-cm^{-1} band (×), and the 1340-cm^{-1} band (▲) in $BChl^{+\cdot}$. The intensities are corrected for self-absorption by using the high concentration correction term of Shriver and Dunn.[42] I_{rs} is the intensity of the Raman scattered light at a particular frequency, and I_s is the intensity of the solvent reference band. λ_{ex} is the excitation wavelength in nanometers. The solid line is the experimental absorption spectrum of BChl cation radical. The molar extinction coefficient axis refers to the absorption spectrum.

(39) Lutz, M.; Kleo, J. *Biochim. Biophys. Acta* **1979**, *546*, 365–369.

on the glass background whose relative intensities do change with exciting wavelength. A more definitive study of these peaks will require experimental conditions which minimize interference from the glass, however.

The Soret region of the $BChl^{+}\cdot$ absorption spectrum is distinctly different from that of $BChl^{0}$. The excellent RR spectra which were obtained at many of the excitation wavelengths provides a better opportunity for comparison with theoretical calculations of the excited electronic states in $BChl^{+}\cdot$ than was afforded by the RR results for $BChl^{0}$. Quantum mechanical calculations of Petke et al.[38] show four strong transitions in the Soret band of $BChl^{+}\cdot$: D_{23}("x") at 411 nm, D_{24}("xy") at 388 nm, D_{26}("x") at 385 nm, and D_{28}("y") at 361 nm. As seen in Table I and in Figure 5, these values are in close agreement with the experimental absorption bands. Good agreement is also observed in the 500-nm region where two transitions are predicted, namely, D_{13}("y") at 525 nm and D_{14}("y") at 519 nm and two are observed experimentally at 502 and 542 nm.

Excitation at 396.7 nm is near the shoulder between the two strong bands in the Soret. From the MO calculations the RR spectra should reflect coupling to the D_{24} and D_{26} transitions. Both involve delocalized π electrons. D_{24} also contains a sizable contribution from ring III with π-electron density at N_3, C_5, and C_4, as well as O_1, the ketone function of ring V. The RR spectrum clearly illustrates strong coupling to the carbonyls (Figure 6). The 1704-cm^{-1} (ketone) and 1674-cm^{-1} (acetyl) vibrations are the most intense ever observed in $BChl^{0}$ or $BChl^{+}\cdot$. Other bands which are strongly resonance enhanced at this wavelength include the 1414- and 1340-cm^{-1} features. These are almost equal in intensity to the methine's at 1597. The 1414-cm^{-1} band is tentatively assigned to a normal mode involving C=C vibrations of the pyrrole rings—especially ring III. This assignment is based on a similar band in Cu porphin and Cu chlorin, as well as the experimental observation that coupling to electronic transitions in $BChl^{+}\cdot$ (D_{24}) and $BChl^{0}$ (S_{11}), both of which contain orbitals with large electron population at C_5 and C_6, show resonance enhancement of the 1414-cm^{-1} band. The band is *not* observed in those spectra obtained by excitation energetically removed from these electronic transitions (such as 457.9-nm CW spectra). The theoretical calculations also lend support to the assignment of the 1340-cm^{-1} band to a normal mode with significant C–N vibrations from the pyrrole rings. D_{24} contains orbital contributions with π-electron density at the N atom in ring III. Finally, the other pronounced feature of the $BChl^{+}\cdot$ spectrum, the shift of the methine peaks to lower frequencies relative to $BChl^{0}$, is also consistent with theory. Calculated spin densities (and experimental values as well[40]) show the α C's (which are adjacent to the methine C's) are the principal centers of spin density. From the experimentally observed shift in the RR vibration, it appears the C=C bond order for the α and methine C's decreases slightly on one-electron oxidation of BChl. Much larger bond order changes are observed in radical ions of small molecules.

The RR spectra obtained with excitation wavelengths farther from D_{23} transition show a large decrease in intensity for all of the vibrations (excepting those in the 950-cm^{-1} region) relative to the methine peak at 1597 cm^{-1}. However, when the excitation wavelength is near the relatively weak transitions at 502 nm in the experimental absorption spectrum, an entirely different RR spectrum is observed. This is expected on the basis of MO calculations showing the nearest transition, D_{14} (519 nm) is "y" polarized. Its lower oscillator strength results in a much weaker RR spectrum. A description of the configurations involved in this transition shows delocalized π-electron orbitals and π-electron density on O_2 and C_{10a}. An explanation for the new peak at 1623 cm^{-1} is not available at this time, but its presence is evidence that a different electronic transition is indeed responsible for resonance enhancement at this wavelength.

3. A Comparison of the RR Spectra of $BChl^{0}$ and $BChl^{+}\cdot$ at Identical Excitation Wavelengths. The RR spectrum of $BChl^{0}$ and $BChl^{+}\cdot$ are distinct at all of the excitation wavelengths used in this study. However, the most dramatic differences are observed for excitation at 396.7 and 416.0 nm. (Excitation at 502.9 nm also gave a weak but distinctive RR spectrum in the case of $BChl^{+}\cdot$, but a satisfactory spectrum of $BChl^{0}$ could not be observed at this wavelength.) Only the most pronounced RR differences between Soret excited $BChl^{+}\cdot$ and $BChl^{0}$ will be discussed here.

(A) **1800–1450 cm^{-1}.** The carbonyl modes are much more enhanced in the 396.7- and 416.0-nm spectra of $BChl^{+}\cdot$ relative to $BChl^{0}$. The 1597-cm^{-1} band is strong and shifted 12 cm^{-1} relative to $BChl^{0}$ at all wavelengths but decreases in intensity less than the 1609-cm^{-1} band in $BChl^{0}$ as the excitation wavelength progresses to red. The smaller decrease in intensity is no doubt the result of strong coupling of this vibration to the 422-nm absorption band. There is no 1530-cm^{-1} band analogous to that in $BChl^{0}$ in any of the $BChl^{+}\cdot$ spectra, as was noted previously in 457.9-nm spectrum.[21]

(B) **1450–950 cm^{-1}.** The intense peaks at 1414 and 1340 cm^{-1} in $BChl^{+}\cdot$ are unique to the 396.7- and 416.0-nm spectra. These bands are only weakly enhanced in the 396.7-nm spectrum of $BChl^{0}$. The 1200–1000-cm^{-1} region is similar in $BChl^{+}\cdot$ and $BChl^{0}$. Enhancement of the two bands near 970 and 950 cm^{-1} is unique to $BChl^{+}\cdot$ at all wavelengths, however.

Conclusions

In summary, the data presented establish several important points. First, it is possible to acquire good quality RR spectra of BChl and its electrogenerated cation radical by using pulsed excitation. The high peak power resulting from pulse half-widths of only 10 ns does not cause detectable photodamage in either the neutral or one-electron oxidized species, as shown by comparing their pulsed and CW spectra. This finding is important for future applications of time-resolved RRS to electron transfer studies in photosynthetic organisms since pulsed excitation is needed in these experiments. Second, the use of SRS as an excitation source has provided laser wavelengths close to, or in resonance with, several electronic states in the Soret region of BChl and $BChl^{+}\cdot$. The changes observed in the RR spectra of both species as a function of excitation wavelength were evaluated relative to recent MO analyses of their excited states. The results suggest that future high-resolution excitation profiles will be valuable for testing these calculations. Theoretical descriptions of the excited states will, in turn, prove helpful in normal-mode analyses of the RR spectra. Third, the RR spectrum of $BChl^{+}\cdot$ is extremely sensitive to excitation wavelength. Two new bands at 1340 and 1414 cm^{-1} were observed in the 396.7- and 416.0-nm spectra. These bands were not seen in spectra recorded by using longer excitation wavelengths, in either the present or previously reported studies,[21,39] and are unique to $BChl^{+}\cdot$. Thus, experimental conditions are now well-defined for detecting $BChl^{+}\cdot$ in the presence of $BChl^{0}$—laser wavelengths may be chosen in the 390–420-nm region to enhance selectively $BChl^{+}\cdot$, and its formation and decay monitored as a function of the 1414- or 1340-cm^{-1} band intensity with time.

Some comment is in order regarding the relevance of the RR spectrum of monomeric $BChl^{+}\cdot$ in solution to the special pair BChl cation radical in the RC. In the latter, electronic coupling between the two molecules in the excited state, as well as electron delocalization in the ground state (assuming the special pair is in the oxidized state throughout the RR experiment), could result in differences in its RR spectrum relative to that of monomeric BChl cation radical. The differences may include intensity changes, which reflect the excited state geometry, and frequency shifts, which reflect the ground state geometry. The magnitude of the differences will depend upon the strength of the intermolecular coupling of the monomer units and the relative orientation of their transition moments. However, from the theoretical analysis of Gregory et al.[41] both the excitation profile and polarization dispersion of given normal mode will be more sensitive to dimerization than the overall RR spectrum, even in the strong coupling limit.

(40) Hoff, A. J.; Mobius, K. *Proc. Natl. Acad. Sci. U.S.A.* **1978**, *75*, 2296–2300.

(41) Gregory, A. R.; Heneker, W. H.; Siebrand, W.; Zgierski, M. Z. *J. Chem. Phys.* **1975**, 5475–5489.

(42) Shriver, D. F., Dunn, J. B. R. *Appl. Spectrosc.* **1974**, *28*, 319–323.

Therefore, it is not unlikely that many of the spectral features observed in the RR spectrum of monomeric $BChl^{+\cdot}$ will be similar to, if not identical with, those of the oxidized special pair BChl in the RC (the 1597-cm^{-1} band has been observed in both cases[39]). Further experiments are planned, by using model systems and RC preparations, to examine in more detail the effects of BChl–BChl interactions on the RR spectrum of the cation radical.

Acknowledgment. The authors wish to thank J. D. Petke, G. M. Maggiora, L. L. Shipman, and R. E. Christoffersen for providing their manuscripts to us prior to publication and Earl Klugman of PARC for the loan of the OMA-2 system. The support of this research by the National Institutes of Health under Grant GM27498-01 and the National Science Foundation under Grant CHE 789-00877 is gratefully acknowledged. In addition, T.M.C. acknowledges support from an NIH Postdoctoral Fellowship and K.D.P. acknowledges support from Eastman Kodak for the 1979–1980 academic year.

Pulsed IR Laser Study of Half-Chair to Boat Interconversion of 2,3-Dihydropyran[1]

Dana Garcia and Ernest Grunwald*

Contribution from the Chemistry Department, Brandeis University, Waltham, Massachusetts 02254. *Received April 29, 1980*

Abstract: At 298 K 2,3-dihydropyran exists largely in the half-chair conformation. Pulsed laser irradiation of the vapor at 1072 cm^{-1}, in the CH_2–O stretching band, produced T jumps to >1400 K. Kinetic UV spectroscopy detected a high-temperature absorption, assignable to the boat form, with λ_{max} = 237 nm and ϵ_{max} (extrapolated to 0 K) = 2.30×10^3 M^{-1} cm^{-1}. Half-chair to boat interconversion, studied at 600–1100 K, gave $\ln K = -1828/T$ and ΔE° = 15.2 kJ/mol. Relaxation times for interconversion were <50 ns. The phenomenology of IR absorption and of the relatively slow retro-Diels–Alder reaction, which occurs at high E_{abs}, is also reported.

Irradiation of gases at pressures above ~5 torr with megawatt IR laser pulses at wavelengths of strong absorption can lead to temperature (T) jumps of over 1000 K on time scales of 4 μs or less. If conditions are controlled so that IR absorption is sufficiently uniform, the T jump is followed by a quiescent period of at least a few microseconds during which the temperature of the irradiated volume can be known.[2] In this paper we use IR laser T jumps to study equilibrium and reaction dynamics for the half-chair to boat interconversion of 2,3-dihydropyran (eq 1).

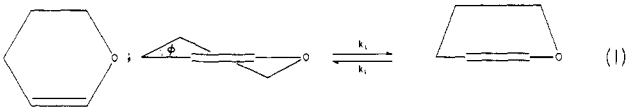

(1)

At room temperature, the dominant form of DHP is the half-chair, as indicated by infrared,[3] Raman,[4] microwave,[5] and NMR[6] spectra. The absence of microwave absorption assignable to the boat form indicates that the proportion of the latter is ≤0.25% (the detection limit)[5] and that $\Delta G^\circ \geq 15$ kJ at 298 K. The angle of twist φ (eq 1) in the half-chair form is 27°, based on microwave data.[5]

Infrared and Raman spectra in the ring-bending and ring-twisting region have been fitted successfully by assuming an effective C_2 molecular symmetry.[3,4] The potential function giving best fit to the spectral data indicates a half-chair minimum with $\varphi = 23°$. Extrapolation of the potential function indicates a second minimum corresponding to the boat form and an intervening barrier of 30 ± 2 kJ/mol.

Low-temperature NMR data yield kinetic constants for the interconversion of the mirror-image conformations of the half-chair form (eq 2).[6] The data are consistent with $k_2 = 10^{13}$ $\exp(-E_{act}/RT)$; E_{act} is 27.6 ± 1.2 kJ/mol, in agreement with the barrier based on IR and Raman data.

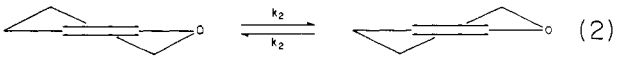

(2)

The ultraviolet absorption spectrum of the half-chair isomer in ethanol at room temperature shows end-absorption only.[7] The vacuum-UV spectrum of the gas shows a longest wavelength peak at 224 nm.[8] Our measurements for the gas at room temperature show a weak shoulder at 224 nm, with molar extinction coefficient $\epsilon \approx 400$ M^{-1} cm^{-1}, and negligible absorption above 230 nm.

Observations Consequent to IR Irradiation. An 8–35-torr sample of 2,3-dihydropyran (DHP) was irradiated at 1072 cm^{-1}, near the peak of the CH_2–O stretch absorption band. The following were measured: absorbed energy per mole (E_{abs}) of DHP, stable reaction products (if any), and transient UV absorption.

When room-temperature DHP (i.e., the half-chair isomer) absorbs at least 20 kJ/mol from a pulsed IR laser, a transient UV absorption appears with band maximum at 237 nm. For reasons given later, it is assigned to the boat form. Typical results for optical transmission vs. time are shown in Figure 1. Three stages of behavior for the IR excited gas are illustrated. The left-hand panel shows the result of the laser-induced T jump. A well-defined plateau is reached after 2 μs, and this quiescent state persists for several microseconds. Somewhat later, in the middle panel, transmission vs. time becomes oscillatory owing to acoustic waves and mixing. These effects eventually subside and the right-hand panel shows the gas cooling back to room temperature.

(1) (a) Work supported in part by a grant from the National Science Foundation and a grant of equipment from the Edith C. Blum Foundation. (b) Based on the Ph.D. Thesis of D.G., Brandeis University, 1980, where further details are published.

(2) Grunwald, E.; Lonzetta, C. M.; Popok, S. *J. Am. Chem. Soc.* **1979**, *101*, 5062.

(3) Lord, R. C.; Rounds, T. C.; Ueda, T. *J. Chem. Phys.* **1972**, *57*, 2572. The authors thank Professor R. C. Lord for a helpful discussion.

(4) Durig, J. R.; Carter, R. O.; Carreira, L. A. *J. Chem. Phys.* **1974**, *60*, 3098.

(5) Williams, V. E. Ph.D. Thesis, University College of North Wales, Bangor, U.K., 1969. Williams, V. E.; Sheridan, J., private communication, July 1979.

(6) Bushweller, C. H.; O'Neil, J. W. *Tetrahedron Lett.* **1969**, *53*, 4713.

(7) Srinivasan, R. *J. Org. Chem.* **1970** *35*, 786.

(8) Planckaert, A. A.; Doucet, J.; Sandorty, C. *J. Chem. Phys.* **1974**, *60*, 4846.

0002-7863/80/1502-6407$01.00/0